DIELECTRIC AND RHEOLOGICAL CHARACTERIZATION OF PHYSICAL GELS BASED ON LIQUID CRYSTALS MIXTURE E7 AND THIOUREA LOW MOLECULAR WEIGHT GELATORS

Muhammed ALKALI [1], Marin MICUTZ[2], Monica ILIȘ[3], Constantin P. GANEA[4], Mihaela RĂDULESCU[5], Viorel CÎRCU [6, *]

This work investigates the gelation behavior and phase stability of E7 liquid crystals using a series of mesogenic benzoylthiourea (BTU) gelators with different alkyl chain lengths (6, 10, 12) at concentrations as low as 2.5 wt.%. Polarized optical microscopy (POM) and differential scanning calorimetry (DSC) confirm that the BTU gelators effectively stabilize the E7/gel composites through hydrogen bonding and π–π interactions. DSC studies reveal a concentration-dependent shift in transition temperatures, with evidence of distinct LC–isotropic and isotropic–gel transitions. Rheological and dielectric studies further demonstrate a reversible gel–sol transition and enhanced dipolar relaxation times (37.7 ns), indicating strong interactions between E7 and the BTU network.

Keywords: liquid crystals, physical gel, low molecular weight gelator, rheology, benzoylthiourea.

1. Introduction

Liquid crystals are inherently fluid and can flow under external forces, which can make them difficult to stabilize in certain applications. The search for methods to stabilize and orient liquid crystals (LC) to make them satisfy technological requirements led to diverse studies over many decades, which largely involved the incorporation of various additives into liquid crystals, thereby modifying them into composite materials. Methods that involve the incorporation

* Corresponding author e-mail: viorel.circu@chimie.unibuc.ro
[1] PhD Student, Dept.of Inorganic and Organic Chemistry, Biochemistry and Catalysis, University of Bucharest, Romania
[2] Assoc. Prof., Dept. of Physical and Analytical Chemistry, University of Bucharest, Romania
[3] Assoc. Prof., Dept. of Inorganic and Organic Chemistry, Biochemistry and Catalysis, University of Bucharest, Romania
[4] Dr., National Institute of Materials Physics, POBox MG 07, Magurele, 077125, Romania
[5] PhD Student, Applied Sciences Doctoral School, National University of Science and Technology POLITEHNICA Bucharest, Romania
[6] Prof., Dept.of Inorganic and Organic Chemistry, Biochemistry and Catalysis, University of Bucharest, Romania, e-mail viorel.circu@chimie.unibuc.ro

of LCs into polymers, such as polymer-dispersed liquid crystals (PDLCs) [1-5] and polymer network liquid crystals (PNLCs) [6-8] have been widely explored among others. In recent years, liquid crystal composites in which the LCs are stabilized by 3-dimensional physical networks are been exploited. These networks are formed by low molecular weight gelators (LMWG), which are organic compounds that have various functional groups that allow them to form gels in the medium of a liquid crystal through non-covalent interactions such as hydrogen bonding and van der Waals forces. The resulting composites obtained from the combination of liquid crystals with gelators form physical gels that combine the unique optical, electro-optical, and anisotropic properties of liquid crystals with the structural and mechanical stability provided by gelators. This hybrid material finds applications in advanced optical devices, sensors, and smart materials. [9]
If the gelator itself has liquid crystalline properties, it adds an additional layer of complexity and functionality to the resulting LC physical gel, potentially leading to unique and enhanced material properties and behaviours. The incorporation of a liquid crystalline gelator can improve the electro-optical performance of the resulting gel. These materials can exhibit enhanced light-scattering effects and faster switching capabilities under an electric field due to better interaction between the liquid crystal solvent and the gelator, [10] for instance, nematic LC gels formed with liquid crystalline gelators have shown lower driving voltages for electro-optical switching compared to those formed with non-liquid crystalline gelators.[11] If the LC gelator is chiral, it can induce unique optical properties such as circular dichroism and enhance chiral recognition in applications like sensors or optical devices. The chirality can lead to helical stacking of molecules, which may further influence the mechanical and optical properties of the gel. [10, 12]

E7 is a widely used nematic LC, known for its favourable thermal and electro-optical properties. When used in physical gels, E7 can maintain its ability to switch between different optical states under an electric field, resulting in improved performance in devices that rely on light modulation and switching. E7 has a well-defined clearing point (at approximately 58 °C). This property enables the formation of gels that can respond dynamically to temperature changes, making them ideal for applications requiring temperature sensitivity or responsiveness. E7 can be effectively combined with various gelators, including low molecular weight compounds or polymers that can self-assemble into fibrous structures, for instance, 1-cyano-trans-1,2-bis(3 ,5 -bis-trifluoromethyl-biphenyl)ethylene [13], 12-hydroxystearic acid [14], and polyfluorene-based π-conjugated polymer, poly(9,9-dioctylfluorene-*alt*-benzothiadiazole) [15] have been used to demonstrate this phenomenon with E7. This compatibility allows for the design of gels with modified properties, such as enhanced mechanical strength or specific thermal behaviors. [15-19]

2. Experimental

Samples preparation. The benzoylthiourea derivatives were prepared according to the procedure described elsewhere. [31] Their chemical structures are presented in Scheme 1. The required amount of the BTU compound was mixed with 0.1 g of E7 liquid crystals mixture supplied by Merck. The mixture obtained was heated to 125ºC followed by slow cooling to room temperature. The formation of the gels was checked by inversion tube method.

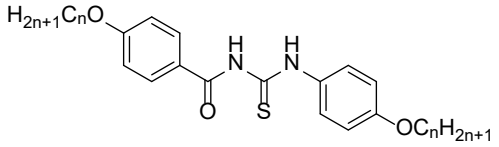

n = 6, *BTU-C6*
n = 10, *BTU-C10*
n = 12, *BTU-C12*

Scheme 1. The chemical structure of the LMWG used in this study.

Dynamic rheology. Oscillatory rheology measurements (frequency sweep tests) were performed on an amount of ~ 0.5 g of sample by employing a rheometer (GBC, VIC, Australia) equipped with a homemade jacket connected to a circulating water bath (Lauda Brinkman Ecoline E100, Suite C Marlton, NJ08053, USA) to ensure discrete and constant working temperatures during investigation. The semisolid sample was carefully sandwiched between the two circular plates parallel to each other (horizontally oriented) of the instrument, with an experimental gap between them of 300 mm. At each temperature value (ranging from 5 to 85^0C – heating phase and back to 5^0C – cooling run with a step of 5^0C) the dynamic rheology tests were carried out by squeezing the sample via a motion of pseudorandom noise shaped profile. In fact, the oscillatory movement vertically oriented was produced by the upper plate with a very small amplitude (0.03-0.04 mm) compared to the value of the gap (thickness of the sandwiched specimen, 300 mm), leading to a corresponding force, through the sample, to the bottom plate below, where a very sensitive sensor recorded it continuously. The displacement and force values acquired during the measurements were processed by a Fourier transform algorithm to provide the experimental values of the storage (G') and loss (G") moduli at 400 individual frequencies simultaneously in the range of 0.25–100.00 Hz, with a step of 0.25 Hz. The measurements were performed in triplicate (with a relative standard deviation of max. 15%), and each rheogram was an average of 30 successive scans.

Dielectric spectroscopy. The dielectric spectroscopy (DS) measurements were performed using a broadband dielectric spectrometer, NOVOCONTROL,

consisting of an Alpha-A high-performance frequency analyzer in the LF domain (0.01 to 107 Hz), equipped with WinDETA software, at a constant ac voltage of 0.5 V. [32, 33] The DS measurements were carried out under isothermal conditions, at a fixed temperature of 27ºC, where the E7 mixture is in the nematic phase.

3. Results and Discussions

Combination of the mesogenic BTU gelators in various concentrations, down to 2.5 (wt. %), all formed white-milky physical gels at room temperature. The morphologies of the different proportions of physical gels were examined by use of textures obtained from polarizing optical microscopy. The images were taken under crossed polarizers at room temperature (gel state), and the textures indicate that the BTU gelator appeared to have stabilized the liquid crystalline phase by restricting molecular mobility, as evidenced by a more uniform texture compared to pure E7, which was fluid and had the characteristic nematic Schlieren texture. For the higher concentrations (10% and 15%) of the BTU, a more prominent alignment of the LC molecules was observed, suggesting that the gelator promotes additional molecular ordering through hydrogen bonding and π-π interactions, while the entangled fibrous network was more visible for the lower gelator (2.5 and 5%) proportions as seen in Fig. 1.

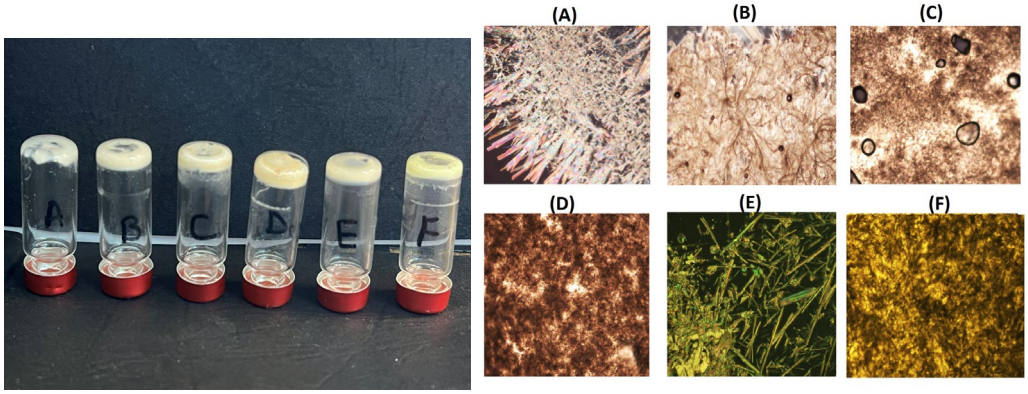

Fig. 1. BTUs physical gel test images (left) and POM textures (right) taken at room temperature: A = *BTU-C12*/E7 (2.5%), B = *BTU-C12*/E7 (5%), C = *BTU-C12*/E7 (10%), D = *BTU-C12*/E7 (15%), E = *BTU-C6*/E7 (10%), F = *BTU-C10*/E7 (10%).

Differential scanning calorimetry (DSC) was employed to investigate the thermal transitions of the mesogenic physical gel. The DSC results corroborate the POM findings, showing that the gelator preserves the thermal and phase behaviour of the E7 liquid crystal. In the first heating cycle, the samples were heated to a maximum temperature of 125 °C (above the clearing point of the pure

BTUs) and subsequently cooled and held at 0 °C for 5 minutes to reform the gel. During this step, there were no characteristic heat changes observed associated with the gelator (Fig. 2). This is an indicator that the BTU alone acts as a physical gelator rather than an LC-forming material. On heating, pure E7 exhibited its characteristic nematic-to-isotropic transition at about 58°C without any intermediate transitions [20] however, in the second and third heating cycles (0-80ºC), just like in the first (0-125ºC), the DSC thermograms (15 and 10 wt%) of the *BTU-C12*/E7 gel on heating, displayed two key transitions, an endothermic peak at about 60ºC and 59.8ºC for 15 and 10 wt% proportions respectively, indicating a LC gel – Iso gel transition (nematic phase of E7 goes into isotropic liquid phase) was observed, closely followed by a broad (approximately 65-70ºC) endothermic peak attributed to an Iso gel – Iso liquid transition (indicating a structural reorganization of the gelator) [11]. This broad peak signifying the structural reorganisation of the gelator gives us an indication that after the E7 becomes isotropic, the BTU gel may continue breaking down further due to disruption in π–π stacking, loss of H-bonding or dissolution of any residual gel-like structures left in the isotropic E7.

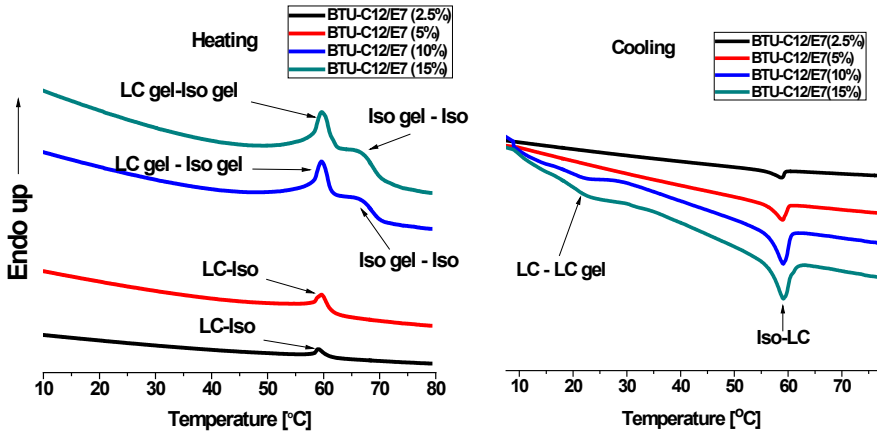

Fig. 2. DSC thermograms of the LC physical gels prepared with *BTU-C12* with various concentrations.

On cooling, a sharp exothermic peak at about 59 °C was seen, indicating an Iso – LC phase transition (reformation of the nematic phase of E7). For the higher concentrations of the gelator (10 and 15 wt.%), a LC–LC gel transition is seen (Fig. 2) in the form of a broad exothermic peak ranging from about 20°C. Observations from the DSC thermograms (Fig. 2) indicates a slight and consistent increase in the LC gel – Iso gel or LC – Iso transitions of the *BTU-C12*/E7 gels, corresponding to the transition to the nematic phase of the E7, with an increase in concentration of the gelator (~59 °C for 2.5%, 59 °C for 5%, 60 °C for 10% and 62ºC for 15%). This trend was also observed on cooling during the reformation of

the nematic phase of E7, the Iso – LC transition temperatures increased steadily with an increase in concentration (at 58, 59, 60, and 61 °C for 2.5, 5.0, 10.0, and 15.0 wt.% proportions, respectively.)

Analogous BTU/E7 gels with 6 carbon atoms in the alkoxy groups (*BTU-C6*) and 10 carbon atoms (*BTU-C10*) on both sides of the BTU were also prepared in a 10% proportion each. Interestingly, the DSC for *BTU-C6* had a distinct pattern (see Fig. 3). On heating, the sharp peak overlapped over a broad transition at 55 °C were assigned to a combination of Iso gel – Iso and LC gel – Iso transitions. Also, upon cooling, two exothermic peaks were seen at 59 and 54°C, which have been assigned to Iso – LC and LC – LC gel, respectively. This situation, where we have the nematic transition peaks appearing at ~55 °C, much lower than for E7, indicates that this BTU gelator (*BTU-C6*) at 10 wt.% concentration disrupts the nematic order of E7, thereby lowering or suppressing the nematic phase transitions. However, 10 wt.% of *BTU-C10* displayed a clear pattern which preserves the properties of E7 just like those of *BTU-C12*.

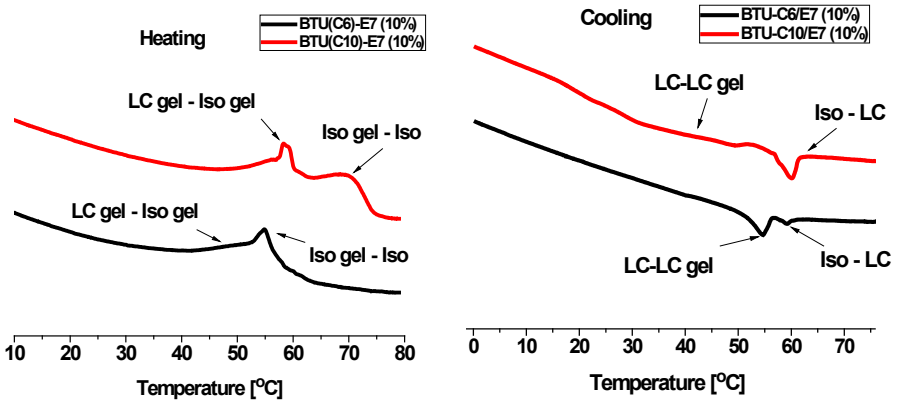

Fig. 3. DSC of the physical gels for *BTU-C6/E7* (10%) and *BTU-C10/E7* (10%).

A representative sample, *BTU-C12*/E7 (10%) was submitted for rheological measurements, and according to the experimental operational parameters employed during dynamic rheological experiment (amplitude of oscillatory motion perpendicularly oriented to the sample – 0.03 mm; gap between rheometer plates – 300 mm), all the rheograms obtained belong to the so-called linear viscoelastic range or region (LVR). Such a linear viscoelasticity associated with a deformable viscoelastic body is essentially founded by Boltzmann's superposition principle: "Each loading step makes an independent contribution to the final state.". [21] This statement, in other words, means that the direct effects exerted by several stresses (loads) onto a sample lead to a strain/deformation, which is a measure of the sum of the applied stresses (loads) taken individually. [22] Practically, within LVR, there is a linear stress-strain dependence (at small

and very small strains), and the microstructure of a sample undergoing this kind of dynamic deformation remains preponderantly unchanged.

Dynamic or oscillatory rheology is well-known as a powerful tool by which the viscoelastic behaviour of a material can be investigated. From this perspective, a gel or gel-like state of a material is always associated with an almost frequency-insensitive evolution of storage modulus (G') and corresponding much smaller magnitude of loss modulus (G") at constant temperature. [23, 24] On the other hand, in a fluid state (exhibiting a viscous behavior) of a material, both G' and G" are frequency dependent and generally G'<G". [23, 25] Additionally, when the two moduli become equal, it is said that the investigated system is at the gel point. [23, 26] The concept of gel point (GP) is a useful quantity which defines the sol-to-gel (SG) or gel-to-sol (GS) transition when a material may undergo such kind of transformation during experiments based on frequency (f), temperature or time sweep. Apart from that, when a viscoelastic system undergoes SG/GS transition as a function of temperature, the values of storage modulus (G') steeply changes (increases in SG transition or decreases in GS transformation) near the transition temperature and the middle of such a steep variation of G' values may indicate the temperature of SG/GS.

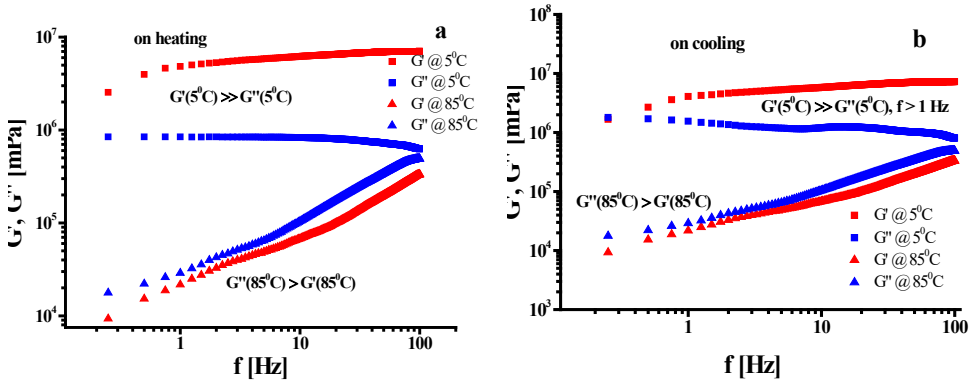

Fig. 4. Frequency evolution of storage and loss moduli acquired at the two limiting temperatures, 5^0C and 85^0C, respectively, (a) on heating and (b) on cooling for *BTU-C12/E7*.

Dynamic rheological measurements were performed on the binary mixture containing E7 (90%, by wt.) and *BTU-C12* (10%. by wt.) displayed a complex viscoelastic behaviour when temperature was swept in the range 5-85^0C, with a step of 5^0C, on both heating and cooling. Thus, the gel-like behaviour noticed at 5^0C (G'>>G" over the entire range of frequency) is totally different from the preponderantly viscous behaviour (G">G') of the same mixture heated at 85^0C (Fig. 4a). Even though the existence of the two limiting states of the system (gel-like and viscous) was obvious, the cooling step slightly reduced the gap between the rheograms G'-f and G"-f taken at 5^0C in the region of low frequencies (Fig.

4b). The intermediate states characterized by the trace's storage and loss moduli vs. frequency acquired at different temperatures are shown in detail in Figs. 5 and 6.

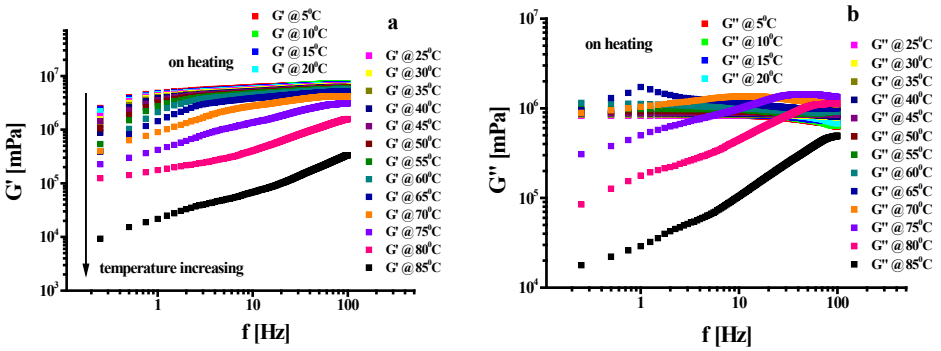

Fig. 5. Rheograms displaying frequency dependencies of (a) storage and (b) loss moduli acquired at heating (5 to 85^{0}C).

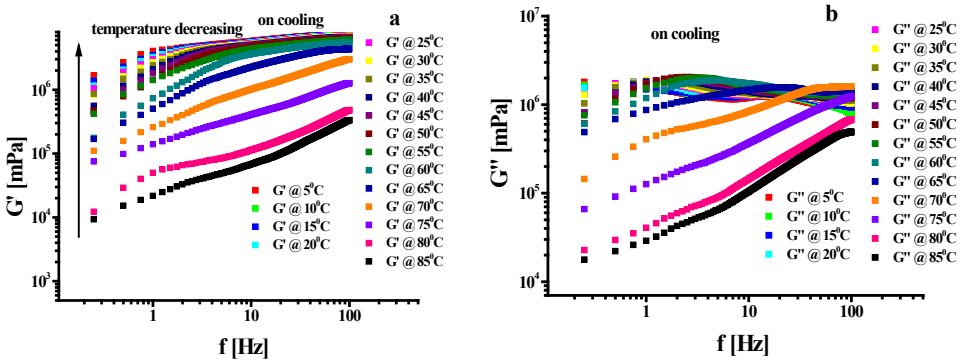

Fig. 6. Rheograms displaying frequency dependencies of (a) storage and (b) loss moduli acquired at cooling (85 to 5^{0}C).

To find out the temperature of the GS and SG transition, we have chosen to consider the temperature evolution of G' at a single frequency of the applied deformation, namely 10 Hz. This is because the reliability of measurements carried out at low frequency (roughly below 1-2 Hz) could be slightly questionable. Thus, the experimental data points distributions resembling the reverse S-shaped (sigmoid) curves storage modulus–temperature were obtained on both heating and cooling, as can be seen in Fig. 7a. By fitting these two sets of experimental data to an equation of Boltzmann-type sigmoid:

$$G' = (G')_{min} + \frac{(G')_{max} - (G')_{min}}{1 + \exp\left(\frac{t - t^*}{b}\right)} \quad (1)$$

where $(G')_{max}$ and $(G')_{min}$ are the highest and lowest fitted values of storage modulus, respectively, t – temperature (in ^{0}C), t* - the GS/SG transition

temperature and b – a parameter (in ^{0}C) which designates the sigmoid steepness. [23] In this context, the abscissae of the inflexion points of the two reverse sigmoidal curves in Fig. 8a (t* = 69^{0}C, R^2 = 0.99004 on heating; t* = 63^{0}C, R^2 = 0.98285 on cooling) are nothing but the temperature of GS transition (at heating) and that of SG transition (at cooling). This behavior with two limiting states (gel-like and viscous fluid) from a rheological standpoint suggests the role played by the BTU component as gelator during the physical (organo) gel formation at temperatures lower than those associated with GS and SG transitions. Moreover, the transition temperatures rheologically detected (69^{0}C on heating and 63^{0}C on cooling) are in satisfactory agreement with the values obtained via DSC (65^{0}C on heating and 60^{0}C on cooling). The differences between these data could be explained by the methods used in studying the thermal material behavior, on one hand, and the way of performing the measurements with temperature (in a static manner, with 15-minute equilibrium thermosetting at every single working temperature – for dynamic rheometry and according to a dynamic regime, where the sample temperature was set to change with a certain rate – for DSC experiments), on the other hand.

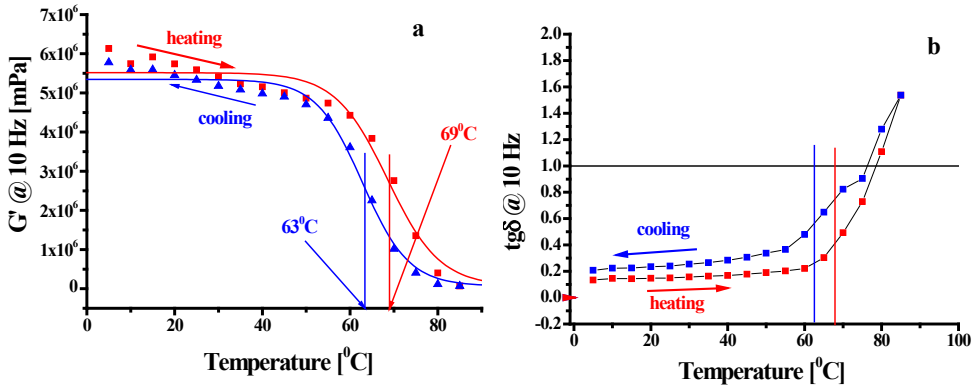

Fig. 7. Temperature dependencies taken at 10 Hz of applied frequency for (a) storage modulus and (b) loss tangent during the processes of heating and cooling.

Another particularly useful, but also intuitive concept in dynamic rheology is known as loss tangent (tgδ), a dimensionless quantity defined as follows:

$$\mathrm{tg}\delta = \frac{G''}{G'} \tag{2}$$

where δ is called the phase angle. The meaning of this quantity arises from what happens with a perfect solid body and an ideal viscous fluid when they experience an external oscillatory strain. Thus, for an ideal solid, both the oscillatory strain and stress recorded are in phase and δ = 0 (in deg or rad). Instead, a perfectly viscous liquid reveals an out of phase by δ = 90^0 = π/2 rad relationship between

strain and stress oscillatory applied. Consequently, the corresponding loss tangent values will be 0 and ∞, respectively. Practically, all real materials lie between the two-limiting behavior, with the phase angle ranging from 0 to 90° ($0^0 < \delta < 90^0$) or within 0 to ∞ an interval when loss tangent is considered ($0 < tg\delta < \infty$). Generally, in the case of gel-like behavior, the elastic (storage) component prevails over that of the energy dissipative (viscous or loss) component, i.e., G' >> G" and the loss tangent tends to have values less than unity, frequently near zero. By taking a liquid-like behavior into account, the viscous component of viscoelastic behavior dominates the elastic one, which means that G" >> G' and, as a result, the loss tangent becomes, more or less, super unitary. At the same time, a viscoelastic material is at gel point when the two viscoelastic moduli, G' and G", are equal each other and $tg\delta = 1$. Based on these considerations, the data plotted in Fig. 7b indicate the presence of gel point at ~ 79^0C on heating and at ~ 76^0C on cooling. Even though these values differ from those obtained by acquiring temperature dependences of storage modulus (Fig. 8a), it is important to state that the equality $tg\delta = 1$ defining the gel point should not be considered an absolute criterion in this respect and highlighting/delimiting the domains of steep variation of the storage modulus with temperature represents a more realistic approach, with higher practical significance. This is all the more so since the values of the transition temperatures (GS and SG) in Fig. 7a actually represent the middle of transition intervals with a certain narrowness. Similar to the case of G' and G" moduli, the intermediate states described by the tgδ - f taken at different temperatures are shown in detail in Fig. 8.

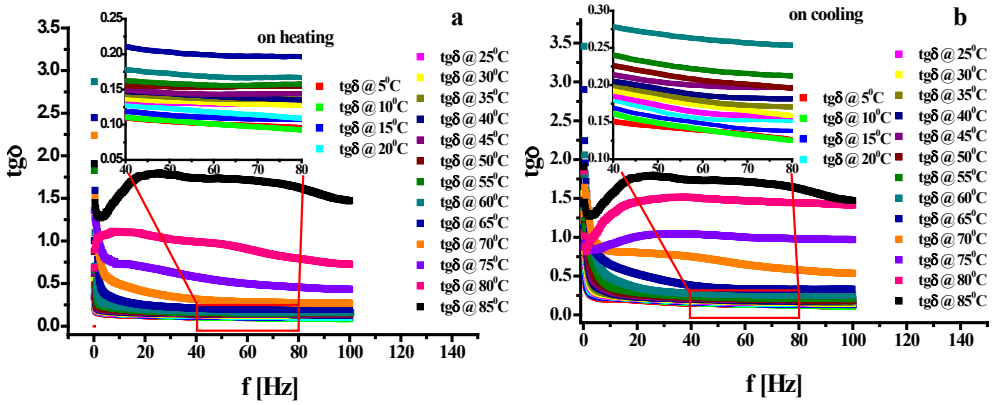

Fig. 8. Loss tangent – frequency dependencies taken (a) at heating and (b) at cooling.

An equally important aspect in this rheological analysis has to do with the strength (given by G' values) and especially the nature of a gel, which can be satisfactorily described by a power law equation of G':

$$G' = K \cdot \omega^n \tag{3}$$

where K and n are two constants and $\omega = 2\pi f$ (in rad/s) is the angular frequency of the strain applied. Equation (3) could be linearized by logarithmation as follows:

$$\log(G') = \log(K) + n \cdot \log(\omega) \quad (4)$$

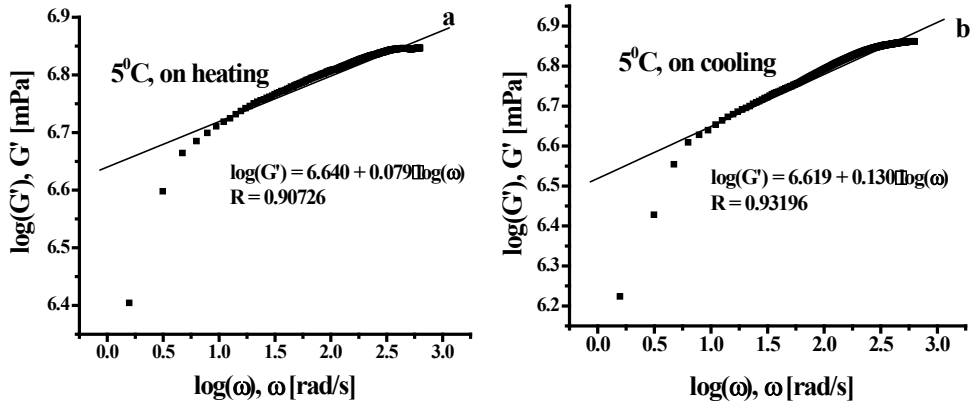

Fig. 9. Fitted experimental values of storage modulus to equation (4) for the physical gel at 5^{0}C during (a) heating and (b) cooling

When the values of coefficient n are zero, the gel is considered a chemical gel (chemically crosslinked), and when n > 0, the gel is a physical one (the crosslinking process is ensured by physical/noncovalent interactions between some chemical entities in the system). Thus, by applying equation (4) to the experimental values of G' obtained at 5^{0}C (on both heating and cooling) (Fig. 9), the two slopes resulting after linear fitting were found to be 0.079 and 0.130 for the gel during the heating run and cooling run, respectively. The values prove practically the as-expected physical nature of the gel-state at the lowest working temperature.

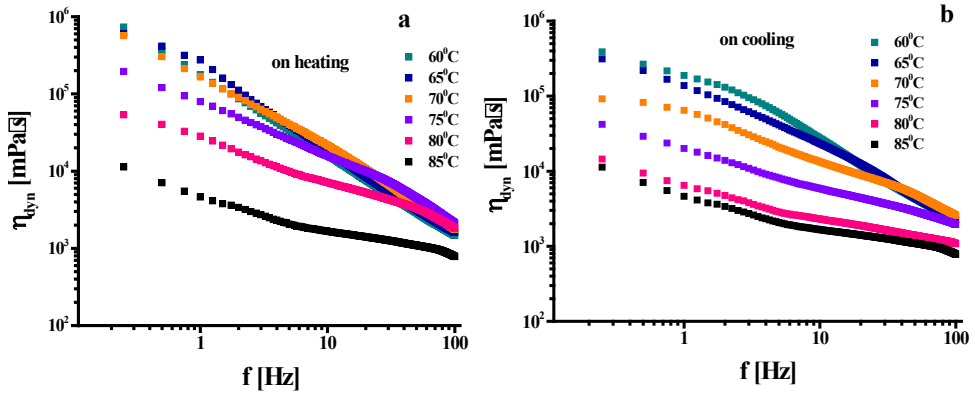

Fig. 10. Dynamic viscosity – frequency dependencies measured (a) at heating (60-85^{0}C °C) and (b) at cooling (85-60^{0}C) in the temperature range where the contribution of the viscous flow component to the viscoelastic behavior of the investigated system is significant.

On a purely practical level, when a material becomes like a gel, it is useless to characterize it using viscosity. But, when the viscous (energy-dissipative) component becomes more and more important in the viscoelastic behavior of a material, the dynamic viscosity defined by the equation below is advisable to be studied.

$$\eta_{dyn} = \frac{G''}{\omega} \tag{5}$$

For the bicomponent system *BTU-C12*/E7, the temperature values at which the energy-dissipative behavior was considered comparable and then exceeding the storage component were in the range 60-85^{0}C (Fig. 10). A comparative analysis of the values of dynamic viscosity measured during the steps of heating-cooling at a single frequency of 10 Hz is graphically illustrated in Fig. 11. At temperatures above those of GS-SG transitions (70^{0}C, 75^{0}C, 80^{0}C), the values of dynamic viscosity acquired on heating are steadily larger than those measured on cooling.

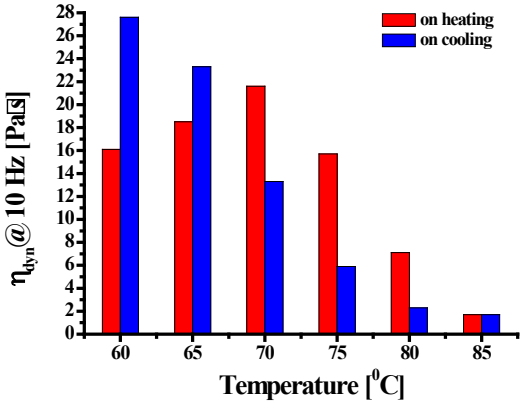

Fig. 11. Comparative diagram illustrating variation of dynamic viscosity at 10 Hz vs. temperature in the range of 60-85^{0}C both on heating and on cooling.

This finding could be indicative of a kinetic process of rearrangement of gelator-E7 molecules during cooling in a sense of far-from-equilibrium states (kinetically speaking) which retain a higher mobility of the molecules with a consequence in maintaining a lower dynamic viscosity for the system (again, on cooling by comparison with those obtained on heating). On the other hand, the situation is totally reversed at the two other lower temperatures – 65^{0}C and 60^{0}C. Practically, h_{dyn} continues to increase with cooling and lowers with temperature decreasing during the heating step. This is in accordance with the existence (or onset) of gel-state at these temperatures corresponding to the heating step and a delayed gel-like behavior for the same system on cooling.

The *BTU-C12*/E7 (5%) gel sample was used for dielectric measurements. The electrical characterization of the sample obtained using the dielectric spectroscopy (DS), can be represented using the complex function of the permittivity $\varepsilon^*(\omega)$ as in eq. (6):

$$\varepsilon^*(\omega) = \varepsilon'(\omega) - i\varepsilon''(\omega) \tag{6}$$

where ε' denotes the permittivity, $\varepsilon''(\omega)$ the dielectric losses. [27]

The dielectric loss tangent is equal to the ratio between the imaginary and the real component of the complex dielectric function:

$$tg\delta_{DS} = \frac{\varepsilon''(\omega)}{\varepsilon'(\omega)} \tag{7}$$

where δ_{DS} is complementary to the phase shift angle. A general model function for the permittivity proposed by Havriliak-Negami is:

$$\varepsilon_{HN}(\omega) = \varepsilon_\infty + \frac{\Delta\varepsilon}{[1+(i\omega\tau_{max})^\alpha]^\beta} \tag{8}$$

where the subunit exponent α, the form factor, takes into account the broadening and flattening of the relaxation process; ε_∞ is relative permittivity value at very high frequencies (ω tends to infinity); $\Delta\varepsilon = \varepsilon_S - \varepsilon_\infty$ is the dielectric strength; ε_S the static permittivity, at $\omega = 0$. We have considered in this study a symmetric shape of the curve β=1, and $\tau_{max} = 1/(2\pi f_{max})$ is the characteristic time, it corresponds to the frequency f_{max} where the dielectric losses have the maximum value.

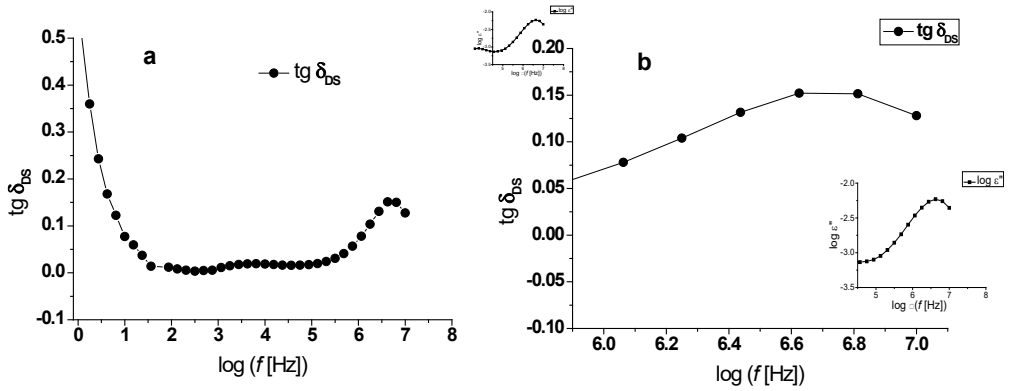

Fig. 12. (a) Loss tangent spectrum for the sample *BTU-C12*/E7 (5%); (b) Dielectric loss tangent spectrum over the interval 1-10 MHz. Inset: Representation of the dielectric loss versus frequency.

Fig. 12a presents the loss tangent spectrum for the sample over the entire frequency range and Fig. 12b shows the variation of the dielectric loss tangent in the high frequency domain 1-10 MHz, where shape of the curve presents a clear maximum. In the inset the dielectric loss spectrum can be seen. The relaxation time obtained is of 3.77 x 10^{-8} s (37.7 ns) and it is attributed to the dipolar relaxation of liquid crystal molecules in the E7/gel composite. Comparing its

value with results obtained for other polymer dispersed liquid crystal composite samples containing the same LC and polymethyl methacrylate, or with E7/cellulose (0.2-4 ns) [28-30], and its value is found to be higher by up to three or four orders of magnitude, due to the stronger interaction between the constituents of the composite.

4. Conclusions

The ability of the benzoylthiourea derivatives having alkoxy chains at both ends to form physical gels with liquid crystals mixture E7 has been investigated by a combination of techniques: DSC, POM, rheological and dielectric spectroscopy measurements. All BTU compounds formed gels in E7 with different thermal behavior related to the alkyl chain length and concentration. The transition temperatures detected by rheology measurements for *BTU-C12*/E7 (10%) gel sample (69^0C on heating and 63^0C on cooling) were in agreement with the values obtained via DSC (65^0C on heating and 60^0C on cooling). The relaxation time of *BTU-C12*/E7 (5%) sample obtained from dielectric measurements was 37.7 ns attributed to the dipolar relaxation of LC molecules in the E7/gel composite. These findings underscore the potential of BTU as LMWG to tailor the structural and dynamic properties of liquid crystal systems for advanced functional applications.

R E F E R E N C E S

[1]. *H. Hakemi*, Polymer Dispersed Liquid Crystal (PDLC) 'Industrial Technology and Devlopment in Europe', Mol. Cryt. Liq. Cryst., Vol. **684**, Iss. 1, 2019, 7–14.

[2]. *W. Gai, Y. Han, M. Zhang, R. Liu, Z. Li, G. Zheng, Z. Fan, Y. Zhang, H. Zhang*, Study on polymer dispersed liquid crystal films with wide viewing angle, Liq. Cryst., Vol. **51**, Iss. 5, 2024, 841–851.

[3]. *H. Lin, Y. Zhao, X. Jiao, H. Gao, Z. Guo, D. Wang, Y. Luan, L. Wang*, Preparation and Application of Polymer-Dispersed Liquid Crystal Film with Step-Driven Display Capability, Molecules, Vol. **29**, Iss. 5, 2024, 1109.

[4]. *H. Zhang, Z. Miao, W. Shen,* Development of polymer-dispersed liquid crystals: From mode innovation to applications, Compos. Part A Appl. Sci. Manuf., Vol. **163**, 2022, 107234.

[5]. *O. Trushkevych, V. Reshetnyak, M. Turvey, R. S. Edwards*, Polymer-dispersed liquid-crystal coatings for ultrasound visualization: Experiment and theory, Phys. Rev. E, Vol**. 109**, Iss. 6, 2024, 064701.

[6]. *B. K. Kim, S. H. Kim, J. C. Song*, Polymer network liquid crystals from UV curable polyurethane acrylate, Polymer, Vol. **39**, Iss. 24, 1998, 5949–5959.

[7]. *Y. Li, Z. Yang, R. Chen, L. Mo, J. Li, M. Hu, S.-T. Wu,* Submillisecond-Response Polymer Network Liquid Crystal Phase Modulators, Polymers, Vol. **12**, 2020, 2862.

[8]. *J. Sun, S.-T. Wu*, Recent advances in polymer network liquid crystal spatial light modulators, J. Polym. Sci. B Polym. Phys., Vol. **52**, Iss. 3, 2014, 183-192.

[9]. *A. S. Sonin, N. A. Churochkina*, Liquid crystals stabilized by physical networks, Polym. Sci. Ser. A, Vol. **55**, Iss. 6, 2013, 353–384.

[10]. *H. Ruan, G. Chen, X. Zhao, Y. Wang, Y. Liao, H. Peng, C.-L. Feng, X. Xie, I. I. Smalyukh,* Chirality-Enabled Liquid Crystalline Physical Gels with High Modulus but Low Driving Voltage, ACS Appl. Mater. Interfaces, Vol. **10**, Iss. 49, 2018, 43184–43191.
[11]. *H. Eimura, M. Yoshio, Y. Shoji, K. Hanabusa, T. Kato*, Liquid-crystalline gels exhibiting electrooptical light scattering properties: fibrous polymerized network of a lysine-based gelator having acrylate moieties, Polym. J., Vol. **44,** 2012, 594–599.
[12]. *T. Kato, Y. Hirai, S. Nakaso, M. Moriyama*, Liquid-crystalline physical gels, Chem. Soc. Rev., Vol. **36**, Iss. 12, 2007, 1857- 1867.
[13]. *X. Tong, J. W. Chung, S. Y. Park, Y. Zhao*, Self-Assembled Liquid-Crystal Gels in an Emulsion, Langmuir, Vol. **25**, Iss. 15, 2009, 8532–8537.
[14]. *H.-C. Lin, C.-H. Wang, J.-K. Wang, S.-F. Tsai,* Fast Response and Spontaneous Alignment in Liquid Crystals Doped with 12-Hydroxystearic Acid Gelators, Materials, Vol. **11**, Iss. 5, 2018, 745.
[15]. *J.-W. Chen, C.-C. Huang, C.-Y. Chao*, Supramolecular Liquid-Crystal Gels Formed by Polyfluorene-Based π-Conjugated Polymer for Switchable Anisotropic Scattering Device, ACS Appl. Mater. Interfaces, Vol. **6**, Iss. 9, 2014, 6757–6764.
[16]. *G. Vijayakumar, M. J. Lee, M. Song, S.-H. Jin,* New liquid crystal-embedded PVdF-co-HFP-based polymer electrolytes for dye-sensitized solar cell applications, Macromol. Res., Vol. **17**, Iss. 12, 2009, 963–968.
[17]. *L. Guan, Y. Zhao*, Self-Assembly of a Liquid Crystalline Anisotropic Gel, Chem. Mater., Vol. **12**, Iss. 12, 2000, 3667–3673.
[18]. *D. Zhao, D. Ouyang, M. Jiang, Y. Liao, H. Peng, X. Xie,* Photomodulated Electro-optical Response in Self-Supporting Liquid Crystalline Physical Gels, Langmuir, Vol. **34**, Iss. 25, 2018, 7519-7526.
[19]. *X. Tong, X. Zhao, Y. Qiu, H. Wang, Y. Liao, X. Xie,* Intrinsically Visible Light-Responsive Liquid Crystalline Physical Gels Driven by a Halogen Bond, Langmuir, Vol. **36**, Iss. 40, 2020, 11873–11879.
[20] *M. Elouali, C. Beyens, F. Z. Elouali, O. Yaroshchuk, B. Abbar, U. Maschke*, Dispersions of Diamond Nanoparticles in Nematic Liquid Crystal/Polymer Materials, Mol. Cryst. Liq. Cryst., Vol. **545**, Iss.1, 2011, 77/[1301]-84/[1308].
[21] *J. Bergstrom*, Mechanics of solid polymers: Theory and Computational Modeling, 1st edition, Amsterdam, Elsevier, 2015.
[22]. *K. Prasad,* Rheology for Chemists - An Introduction, Appl. Rheol., Vol. **16**, Iss. 2, 2006, 69.
[23]. *T. Staicu, M. Iliş, V. Cîrcu, M. Micutz,* Influence of hydrocarbon moieties of partially fluorinated N -benzoyl thiourea compounds on their gelation properties. A detailed rheological study of complex viscoelastic behavior of decanol/ N-benzoyl thiourea mixtures, J. Mol. Liq., Vol. **255**, 2018, 297–312.
[24]. *H. B. Bohidar, P. Dubin, Y. Osada*, Eds., Polymer Gels: Fundamentals and Applications, ACS Symposium Series, Vol. **833**, Washington, DC: American Chemical Society, 2002.
[25]. *C. J. Chern, E. Beutler*, Biochemical and electrophoretic studies of erythrocyte pyridoxine kinase in white and black Americans, Am. J. Hum. Genet., Vol. **28**, Iss.1, 1976, 9–17.
[26]. *M. V. Neacsu, I. Matei, M. Micutz, T. Staicu, A. Precupas, V.T. Popa, A. Salifoglou, G. Ionita,* Interaction between albumin and pluronic F127 block copolymer revealed by global and local physicochemical profiling., J. Phys. Chem. B, Vol.**120**, 2016, 4258–4267.
[27]. *D. Manaila-Maximean, M. Ilis, P. C. Ganea, M. Micutz, C. Boscornea, V. Cîrcu*, Dielectric characterization of polymer dispersed liquid crystal film with chitosan biopolymer, J. Mol. Liq., Vol. **393**, 2024, 123552.

[28]. *L. F. Chiriac, P. C. Ganea, D. M. Maximean, I. Pasuk, V. Cîrcu*, Synthesis and thermal, emission and dielectric properties of liquid crystalline Eu(III), Sm(III) and Tb(III) complexes based on mesogenic 4-pyridone ligands functionalized with cyanobiphenyl groups, J. Mol. Liq., Vol. **290**, 2019, 111184.
[29]. *F. Kremer, A. Schönhals,* 2003, Molecular and Collective Dynamics of (Polymeric) Liquid Crystals, 385-432, In: F. Kremer, A. Schönhals, (eds) Broadband Dielectric Spectroscopy. Springer, Berlin, Heidelberg
[30]. *C. P. Ganea, D. Manaila-Maximean, V. Cîrcu*, Dielectric investigations on carbon nanotubes doped polymer dispersed liquid crystal films, *Eur. Phys. J. Plus*, Vol. **135**, Iss. 10, 2020, 797.
[31]. *M. Ilis, M. Bucos, F. Dumitrascu, V. Circu*, Mesomorphic behaviour of N-benzoyl-N′-aryl thioureas liquid crystalline compounds, J. Mol. Struct., Vol. **987**, Iss. 1-3, 2011, 1-6.
[32]. *D. M. Maximean, O. Danila, P. L. Almeida, C. P. Ganea*, Electrical properties of a liquid crystal dispersed in an electrospun cellulose acetate network, Beilstein J. Nanotechnol., Vol. **9**, 2018, 155–163.
[33]. *D. M. Maximean, O. Danila, C. P. Ganea, P. L. Almeida*, Filling in the voids of electrospun hydroxypropyl cellulose network: Dielectric investigations, Eur. Phys. J. Plus, Vol. **133**, Iss. 4, 2018, 159.